Fashion and Textiles

RESEARCH

Open Access

Characterization of antioxidant *Houttuynia cordata* extracts loaded polyurethane nanofibers

Mei Xi Chen[1†], Md. Kaiser Haider[2†], Ick Soo Kim[2*] and Jung-Soon Lee[1*]

[†]Mei Xi Chen and Md. Kaiser Haider contributed equally to this work and are first authors

*Correspondence: kim@shinshu-u.ac.jp; jungsoon@cnu.ac.kr

[1] Department of Clothing and Textiles, College of Human Ecology, Chungnam National University, 99 Daehak-ro, Yusung-gu, Daejeon 31434, South Korea

[2] Nano Fusion Technology Research Group, Institute for Fiber Engineering (IFES), Interdisciplinary Cluster for Cutting Edge Research (ICCER), Shinshu University, Tokida 3-15-1, Ueda, Nagano 386-8567, Japan

Abstract

Herein, we analyzed total polyphenol content, total flavonoid content, and the antioxidant activity of the ethanol and distilled water extracted *Houttuynia cordata* perennial herb. Later, we investigated the possibility of producing *Houttuynia cordata* extract (HCE) loaded Polyurethane (PU) nanofibers via the electrospinning technique. The analysis confirmed that the total polyphenol, total flavonoid content, and antioxidant activity of the ethanol extracted HCE were higher than the distilled water extracted HCE. Therefore, the ethanol extracted HCE was used to prepare HCE/PU nanofibers by varying concentrations of HCE and PU. The HCE/PU nanofibers showed a mixed pattern of beads and fibers at a PU concentration of 10 wt%. However, at 12 wt% PU concentration, relatively uniform nanofibers with an average diameter of about 200 nm were formed at 1.0% and 1.5 wt% of HCE. The successful incorporation of HCE in PU nanofibrous matrix was confirmed by the presence of its characteristic bands in Fourier transform infrared (FTIR) and X-ray diffraction (XRD) spectra. The addition of HCE increased the crystallinity, the amount of heat required for pyrolysis, and the thermal stability of HCE/PU nanofibers, which must be credited to the HCE-derived quercitrin and quercetin crystallite solids.

Keywords: *Houttuynia cordata* extract (HCE), Polyurethane (PU), HCE/PU nanofiber, Ethanol extract, Antioxidant activity

Introduction

The continuous exposure of living cells, either human, animal, or plant species, to various challenges exerts oxidative stress. Alternatively, oxidative stress could be produced from exogenic sources like continuous exposure to toxic pollutants and ionizing irradiation. The severity of the induced oxidative stress in a biological system can be manifested from the diagnosis of increased exposure to oxidants or a decrease in the antioxidant capacity of the system (Chevion & Chevion, 2000). Although the mechanism and effectiveness of the defense system of living cells are strong, inappropriate handling of biologically operated transition metal ions, such as iron and copper may lead to the generation of highly reactive free radical species, which are capable of damaging almost everything found in the human body (Halliwell, 1997). Furthermore, study revealed that

the living tissues undergo excessive oxidative stress while extracellular matrix alike scaffold-supported regeneration of the tissues. Thus, there is an acute need for the preparation of scaffolds with antioxidant activity that may suppress the induced oxidative stress throughout the tissue regeneration process (Li et al., 2013).

The advancement of nanotechnology broadens the ideology regarding a wide range of applications, such as textiles, biomedicine, medical textiles, energy storage system, effluents treatment, catalysis, etc. (Gotmare et al., 2018; Haider et al., 2021; Ullah et al., 2021). Nanofibers are one of the most significant outcomes of nanotechnology and their application area is increasing day by day owing to their use compatibility. Nanofibers can be produced by a wide range of techniques, for example, template synthesis, drawing, phase separation, melt-blown technology, electrospinning, centrifugal spinning, etc. (Almetwally et al., 2017). Among them, electrospinning is considered a most effective method of preparing nanofibers due to its easy operational technique, ease of fiber functionalization, compatibility of using a wide range of polymers, ease of fiber deposition, and structural designing, and mass production capability (Feng et al., 2019; Kwak et al., 2017).

The extracellular matrix alike structure of the electrospun nanofibers makes it a lucrative material for tissue engineering scaffolds. A large number of research has been published on nanofiber-based regenerative therapies in the last several years. Among them, nanofibers with antioxidants are a particular area of interest. Yang et al. (2016) prepared PVA/Tannic acid/ Fe^{3+} hybrid nanofibers with high antioxidant activity and mechanical stability. Zhou et al. (2016) prepared layer-by-layer cellulose nanofibrous film cast with polyphenolic tannic acid/polyethylene glycol, which exhibited long-lasting antioxidant activity in both 2,2-diphenyl-1-picrylhydrazyl (DPPH) and 2,2′-azino-bis (3-ethylben zothiazoline-6-sulfonic acid) diammonium salt (ABTS) radical scavenging test. Lee et al. (2017) prepared pullulan nanofiber by compositing it with plant-derived flavonoid-based antioxidant rutin. The Pristine rutin and rutin/pullulan nanofibers displayed equal 80% antioxidant activity at 10 mg/mL rutin concentration by ABTS test. Polymeric nanofibers with excellent antioxidant activity were produced from porphyrin, green tea extract, rice extracts, *Garcinia mangostana* extracts, etc. as active substances (Arai et al., 2012; Chuysinuan et al., 2017; Pusporini et al., 2018; Sriyanti et al., 2017).

Houttuynia cordata (HC) is a flowering perennial herb that belongs to the Saururaceae family and is native to Korea, Japan, China, and Southeast Asia. It contains two stoloniferous rhizomes having two distinct chemotypes (Brown, 1995). It is a well-known traditional medicine in the indigenous medical care of Southeast Asia. Owing to numerous medicinal values, the extraction of the active components of HC is a great concern. A wide range of extraction methods was employed to extract polyphenols and flavonoid components of HC, including Soxhlet extraction, ultrasonic extraction, ethanol/methanol extraction, pressurized liquid extraction, Ethanol/acetone extraction, microwave-assisted extraction, etc. (Fu et al., 2013). Researchers reported and quantified six different flavonoid glycosides contained in HC, namely—hyperin, quercitrin, quercetin, rutin, afzelin, and isoquercitrin, in particular, a large quantity of crystalline quercitrin is present in HC (Xu et al., 2006). Hence, it is expected that abundant antioxidant-containing HC could be used as a regenerative medicine by encapsulating it into polymeric nanofibers. Such nanofibers are anticipated to release HC-derived active compounds in

the specific target area under concern and suppress the oxidative stress-induced malfunctioning of living cells, thus protecting cell activity and proliferation.

The formation of different polymeric nanofibers containing different active compounds via electrospinning is not new, however viable loading concentration of HC extracts in electrospun PU nanofibers to achieve uniform nano morphological structures along with physio-chemical and thermal property was not revealed in earlier studies. Therefore, in this study, HC was extracted by organic and water as solvents, and the main antioxidant components: phenolic and flavonoid contents are quantified. The antioxidant activity of HCE was evaluated by DPPH and ABTS radical scavenging test. To evaluate the electrospinnability of HCE with polymeric nanofibers, HCE having better antioxidant potential was employed to prepare HCE/PU nanofibers via the electrospinning technique. The concentration of HCE and PU polymer was optimized by observing the morphology of the produced PU and HCE/PU nanofibers. The chemical interaction and crystallinity of HCE/PU nanofibers were examined by Fourier Transform Infrared Spectroscopy and X-ray diffraction analysis. Finally, the thermal decomposition behavior of the produced nanofibers was evaluated by Differential Scanning Calorimetry and Thermogravimetric analysis. Our findings demonstrated that HCE can be successfully incorporated into PU polymeric nanofiber matrix via electrospinning without any significant negative effect on fiber characteristics, however further in-vitro and in-vivo characterizations are obligatory.

Methods

Materials

Commercially available dried *Houttuynia cordata* was purchased and used. Tertiary distilled water (H_2O) and 99.9% ethanol (C_2H_5OH) were used. Polyurethane (PU, pellethane 2103-80AE, MW = 80,000) was obtained from Lubrizol (USA), and *N*-dimethylformamide (DMF, > 98%) was purchased from Daejung Chemicals (Korea). Folin & Ciocalteu's phenol reagent, tannic acid (ACS reagent), potassium acetate (≥ 99.0%), quercetin (≥ 95%), 2,2-diphenyl-1-picrylhydrazyl (≥ 95%), 2,2′-azino-bis (3-ethylben zothiazoline-6-sulfonic acid) diammonium salt (≥ 98.0%), and potassium persulfate (≥ 99.0%) were purchased from Sigma Aldrich (USA). Sodium carbonate (99.0%) and aluminum nitrate (99.0%) were purchased from Samchun Chemicals (Korea).

Extraction of *Houttuynia cordata*

The HCE was extracted using 99.9% ethanol and distilled water as solvents. For the ethanol extraction method, dried *Houttuynia cordata* and ethanol were immersed in a beaker at a liquor ratio of 1:20 for 48 h at room temperature. After filtration with filter paper, the same process was repeated two times. For DW extraction method, dried *Houttuynia cordata* was poured into distilled water at a ratio of 1:20 and heated for 60 min at 100 °C. After filtration, the obtained extract was subjected to the same process two times. After that, the resultant extracts were filtered three times with a filter paper until there was no precipitate left in the extracted solution. The obtained extracts were concentrated into the gummy state by using a rotary evaporator (RV10, IKA®, Germany) at 60 °C with a rotation speed of 50 rpm. The gummy extracts were further diluted and used.

Preparation of HCE/PU nanofibers via electrospinning

At first, a 10 wt% PU polymer solution was prepared by using DMF as solvent (Woo & Lee, 2021). After stirring for 12 h and ultrasonication for 1 h, 0.5, 1.0, 1.5, and 2.0 wt% ethanol extracted HCE were added to the resultant PU solution and stirred for 12 h for homogeneous mixing of the blends. Similarly, a 12 wt% PU polymer solution was prepared with 0.5, 1.0, 1.5, and 2.0 wt% ethanol extracted HCE. Electrospinning was done at a voltage of 15 kV, a tip-to-collector distance of 15 cm, and a flowrate of 0.3 mL/h.

Determination of total polyphenol and flavonoid contents

The total polyphenol content of HCE was measured by modifying the Folin-Denis method (Hillis & Swain, 1959). 0.2 mL *HCE* was diluted to 1 mg/mL with 0.2 mL of Folin & Ciocalteu's phenol reagent at room temperature for 3 min. Then, 3 mL of 10% sodium carbonate solution was added to the mixture and reacted in a dark room for 1 h until the components were mixed properly. The resultant solution was subjected to the absorbance measurement at 745 nm using a spectrophotometer. The total phenolic content was obtained through extrapolation of obtained absorbance from the standard curve of serially diluted tannic acid of concentrations 15.625, 31.250, 62.500, 125.000, and 250.000 μg/mL against the corresponding absorbance. The total flavonoid content was measured by modifying the method of Moreno et al. (2000). After mixing 0.4 mL of 80% ethanol to 0.1 mL of *HCE* diluted to a concentration of 10 mg/mL, 0.1 mL of 10% aluminum nitrate solution, 0.1 mL of a 1 M potassium acetate solution, 4.7 mL of 80% ethanol were added and reacted for 40 min. A spectrophotometer was used to measure the absorbance of the reacted solution at a wavelength of 415 nm. The total flavonoid content was obtained through extrapolation of obtained absorbance from the standard curve of serially diluted quercetin of concentrations 62.5, 125.0, 250.0, and 500.0 μg/mL against the corresponding absorbance.

DPPH and ABTS radical scavenging activity measurement

The DPPH free radical scavenging assay was conducted to evaluate the antioxidant activity of the HCE. The DPPH radical scavenging activity was measured by the method of Kim et al. (2018). After diluting HCE to a concentration in the range of 1–4 mg/mL, 0.1 mL of the *HCE* was mixed with 1 mL of a 0.4 mM DPPH solution. After that 1.4 mL of ethanol was added, and the mixture was reacted for 30 min in a dark room. A spectrophotometer was used to determine the absorbance of the reacted solution at a wavelength of 517 nm. The following Eq. (1) was used to calculate the DPPH radical scavenging ability.

The ABTS radical scavenging ability was measured by the method of Kim et al. (2018). At first, 14 mM ABTS and 4.9 mM potassium persulfate solutions were mixed at the ratio of 1:1 (v/v) and reacted in a dark room for 12 to 16 h, after which the mixture was diluted with distilled water to have an absorbance value of 0.7 to 0.8 at 734 nm. We added 0.05 mL of *HCE* diluted to a concentration of 1 to 4 mg/mL using 0.95 mL of the diluted $ABTS^{+}$ solution, followed by measuring the absorbance after 10 min. Equation (1) was used to calculate the ABTS radical scavenging activity:

$$\text{Radical scavenging activity}(\%) = \left(1 - \frac{\text{A}s}{Ac}\right) \times 100 \quad (1)$$

where A*s* is the absorbance of the solution with HCE and A*c* is the absorbance of the solution without HCE.

Surface morphology of the produced HCE/PU nanofibers

A scanning electron microscope (SEM) (JSM-6010LA, JEOL, Japan) with 10 kV acceleration voltage was used to investigate the surface morphology of the produced nanofibers. All the nanofibrous were sputtered coated with Platinum (Pt) for 120 s at 20 mA before SEM observation. The diameter of the nanofibers was measured from the obtained SEM images by employing Image J 1.50i software and Excel, and the results were displayed in average values. The average diameter of the nanofibers was calculated over 200 nanofiber strands for each specimen.

Physicochemical analysis

FTIR Spectrometer (ALPHA-P, Bruker, Germany) between the wavenumber range 500 cm^{-1} to 4000 cm^{-1} was used to examine the changes in the chemical structure of the nanofibers and the interaction between PU and *HCE*.

XRD analysis

The influence of the addition of HCE in the crystal structure of PU polymeric nanofiber matrix was measured by using a High-resolution X-ray Diffractometer (AXS, Bruker, Germany). The analysis was carried out under the conditions of 40 kV and 40 mA using Cu Kα as an X-ray tube. The diffractometer was set to measure between the 2θ range of 5–80° at a stepwise rate of 0.5°/s.

Thermal degradation analysis

The thermal degradation behavior of the produced nanofibers was measured by using a thermal analyzer (TGA/DSC 1, Mettler-Toledo, Korea). The thermal degradability was measured between a temperature range of 25 °C to 800 °C under a nitrogen gas atmosphere at a heating rate of 10 °C/min.

Results and Discussion

Total polyphenol and flavonoid contents

Polyphenols, including flavonoids, are secondary metabolites contained in almost all parts of the plant. These are strong antioxidants that can effectively scavenge free radicals thereby protecting living cells from harmful free-radical initiated oxidation. Antioxidant polyphenols, especially flavonoids, are potential inhibitors of low-density lipoprotein (LDL) oxidation. Through the different antioxidant mechanisms of action, polyphenols show their protective effect against cardiovascular disease. Besides, flavonoids have antithrombotic, vasoprotective, and hypolipidemic effects (Bravo, 1998). Many studies reported that quercitrin, a phenolic component that exists in *Houttuynia cordata*, has excellent and faster free radical scavenging activity. The total amount of phenolic compounds, such as flavonoids,

phenolic acids, and anthocyanins was evaluated for their antioxidant activity by DPPH radical scavenging activity (Jeong et al., 2008). The total polyphenol content of ethanol and DW extracted HCE was measured to be 577.10 ± 13.58 mg/g and 435.99 ± 3.80 mg/g, respectively. Besides, the total flavonoid content was measured to be 551.16 ± 64.28 mg/g for the ethanol extracted HCE and 266.19 ± 23.35 mg/g for DW extracted HCE. The total polyphenol content and the total flavonoid content of the ethanol extracted HCE were about 1.3 times and 2 times higher than those of the DW extracted HCE, respectively. Such findings must be credited to quercitrin of HCE, a polyphenolic compound that does not dissolve well in water but is slightly soluble in ethanol (Jeong et al., 2010). Studies revealed that organic solvent-based extraction is more efficient in extracting valuable components than water-based extraction and the extraction yield of flavonoids is higher when the extraction is carried out using organic solvents than water-soluble solvents (Choi et al., 2003).

DPPH and ABTS radical scavenging ability

DPPH radical scavenging activity is a method widely used to measure the antioxidant activity of compounds containing phenolic and aromatic amine compounds. The DPPH free radical upon acceptance of an electron from the flavonoids in HCE changes its color to yellowish. This difference was colorimetrically measured using a UV–Visible spectrophotometer, and radical inhibition was measured.

By using the characteristic of changing from purple to colorless at 517 nm, it can be used as a criterion to measure not only lipid oxidation but also aging inhibition by free radicals generated in in-vivo metabolism. ABTS radical scavenging activity is a method used to measure antioxidant activity against hydrophilic and lipophilic substances, and both chain-blocking antioxidants and hydrogen-donating antioxidants can be measured. The principle of ABTS radical scavenging activity measurement is a process in which ABTS exhibits a blue-green color due to electron oxidation by potassium persulfate, and then the blue-green color gradually fades as the electron-donating ability is reduced by the antioxidant contained in the extract. It is known as a method that can confirm antioxidant activity more sensitively than the DPPH radical scavenging method (Choi et al., 2003).

Figure 1 shows the results of DPPH and ABTS radical scavenging activity of *Houttuynia cordata* extract. A linear increment in the DPPH radical scavenging ability was observed with the increase in HCE concentration for both ethanol and DW extracted HCE. In case of DPPH scavenging test, the antioxidant activity of ethanol extracted HCE was calculated between 9.36 and 42.11%, while for DW extracted HCE between 7.92 and 35.32%. A more prominent antioxidant activity of the HCE was observed in case of ABTS scavenging test than in the DPPH test. In ABTS scavenging test, the ethanol extracted HCE displayed an antioxidant activity between 32.07 and 99.99%, while for DW extracted HCE ranges between 29.22 and 77.53%. These findings also indicate more susceptibility of the ABTS scavenging test and the superiority of organic solvent-based extraction over the water-based extraction method. Thus, we used ethanol extracted HCE to prepare HCE/PU nanofibers via electrospinning.

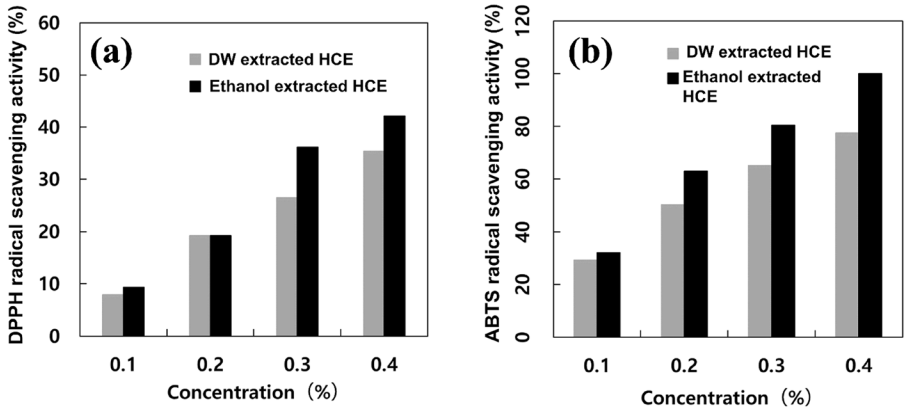

Fig. 1 **a** DPPH and **b** ABTS radical scavenging activity of HCE

Morphological analysis of the HCE/PU nanofibers

The morphology of the pristine PU (10 wt%) and HCE/PU nanofibers are depicted in Fig. 2. The pristine PU nanofibers displayed beaded morphology with fibers embedded with large spherical beads. Although the incorporation of HCE reduces the tendency of bead formation, beads were present at varying concentrations of HCE. The morphology of pristine PU (12 wt%) and HCE/PU nanofibers are shown in Fig. 3. Large spherical beads were formed in pristine PU nanofibers. However, the propensity to bead formation in HCE/PU nanofibers was significantly reduced. Very few beads were formed in HCE/PU nanofibers with 0.5 wt% HCE. With a further increment in the addition of HCE concentration to 1.0 and 1.5 wt%, beads disappeared and uniform continuous nanofibers were formed. The formation of beads in nanofibers while electrospinning depends on many different factors, such as polymer type, concentration, viscosity, conductivity, flow rate, relative humidity, etc. Beadless nanofibers at 12wt% PU concentration are formed by earlier published reports (Yang et al., 2010). Also, it was demonstrated that the flow rate is a major fact for beadless fiber formation of PU polymer via electrospinning. The increase in the flow rate of polymer solution causes more quantity of polymer to reach on the tip of needle, therefore effecting accurate Taylor cone formation, thus causing to form beads on the spun nanofibers. More accurately, an increase in the flow rate creates obstacles for stretched polymers/fibers to completely dry before they reach the collector. Therefore, when nanofibers are flowing towards collector soft undried segments stretched more while hard segments stretched less, thus causing formation of beads on the ultimate nanofiber. Thus, we assumed that the incompatibility in the polymer concentration and the flow rate at the set electrospinning parameters might be the reason for the formation of beads in the pristine PU nanofibers. Moreover, in HCE/PU nanofibers, reduced tendency of bead formation can be ascribed to the reduced viscosity of the electrospinning solution by the addition of ethanol extracts of 1.0 and 1.5 wt% HC. The HCE/PU solution might achieve a proper viscous property at the set electrospinning parameters, thereby causing to form uniform nanofibers. The diameter distribution histograms of HCE/PU nanofibers are depicted in Fig. 4. Relatively uniform nanofibers with an average diameter of about 178 nm, between 50 and 450 nm diameter distribution range

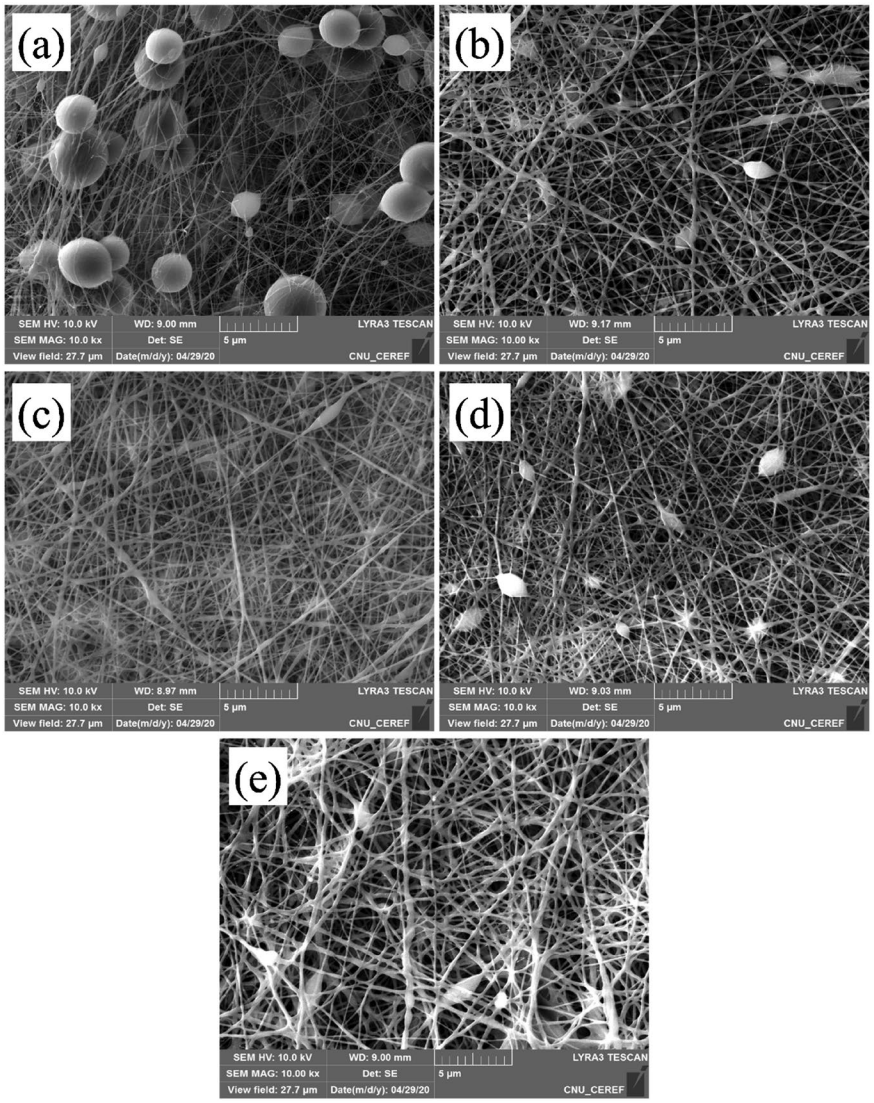

Fig. 2 SEM micrographs of HCE/PU nanofibers (10 wt% PU concentration) with different HCE concentrations: **a** 0 wt%, **b** 0.5 wt%, **c** 1.0 wt%, **d** 1.5 wt%, and **e** 2.0 wt%

were produced at 0.5 wt% HCE concentration. At 1.0 wt% concentration of HCE, the average diameter of the nanofibers increased without any changes in the diameter distribution range. At 0.5 and 1.0 wt% concentration of HCE, the inclusion of HCE inside nanofibers might cause such increase in the diameter of the nanofibers. With a further increase in the concentrations of HCE to 1.5 and 2.0 wt%, the diameter distribution range was contracted with a linear decrease in the average diameter of the nanofibers. The increased viscosity of HCE/PU solution at 1.5 and 2.0 wt% of HCE caused increased stretching of the polymer jet, thus resulting a reduction in the average diameter of the nanofibers. Besides, some irregularity was identified in 2.0 wt% HCE-loaded PU nanofibers. The average diameters of the nanofibers with 1.5 and 2.0 wt% HCE concentrations were calculated to be 193 nm and 186 nm with the diameter distribution range between 75 and 360 nm and 50 and 400 nm, respectively. Such

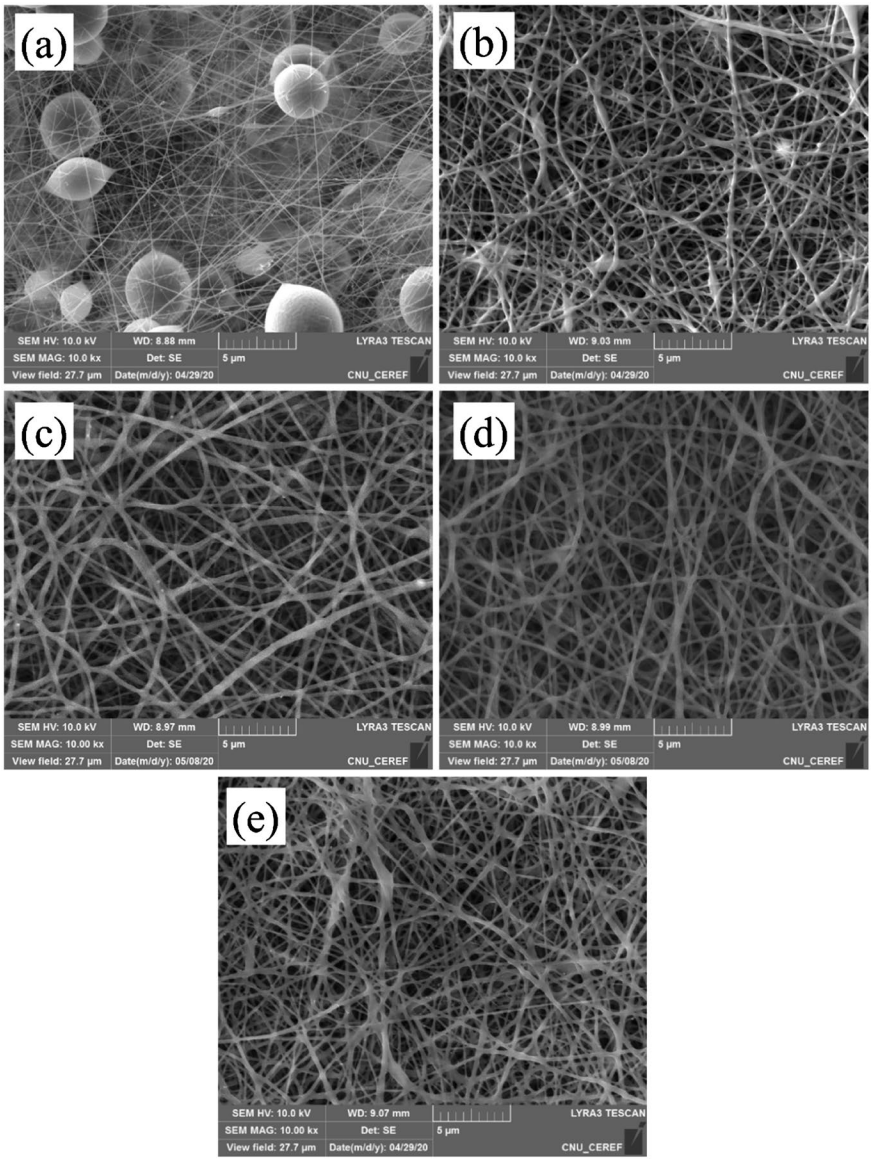

Fig. 3 SEM micrographs of HCE/PU nanofibers (12 wt% PU concentration) with different concentrations of HCE: **a** 0 wt%, **b** 0.5 wt%, **c** 1.0 wt%, **d** 1.5 wt%, and **e** 2.0 wt%

findings indicate that bead-free and uniform HCE/PU nanofibers can be formed at 1.0 and 1.5 wt% concentrations of HCE.

Chemical interaction analysis

The ATR fingerprints of neat PU and HCE/PU nanofibers are displayed in Fig. 5. The pristine PU nanofibers exhibited different characteristics peaks at 3334 cm^{-1} for NH stretching vibration, at 2953 cm^{-1} for CH asymmetric vibration, at 2895 cm^{-1} for CH symmetric vibration, at 1725 cm^{-1} and 1706 cm^{-1} for carbonyl stretching of urethane groups (Akduman et al., 2016), at 1529 cm^{-1} for –NHCOO– vibration, at 1414 cm^{-1} for CH_3 bending vibration, at 1218 cm^{-1}, 1167 cm^{-1}, and 1069 cm^{-1} for stretching vibrations of ester linkages (Da Silva et al., 2009; Unnithan et al., 2015).

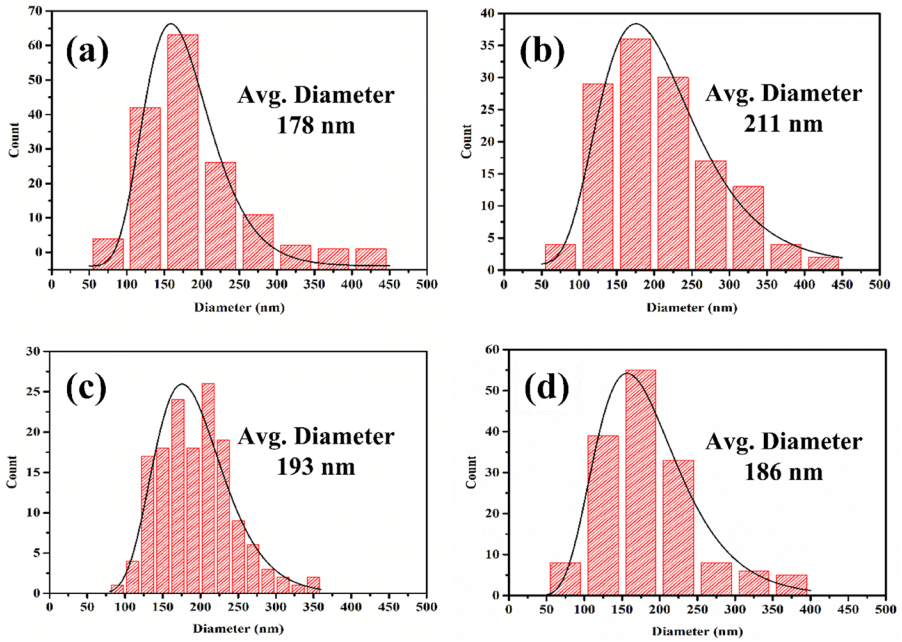

Fig. 4 Diameter distribution histograms of HCE/PU nanofibers (12 wt% PU concentration) with different concentrations of HCE: **a** 0.5 wt%, **b** 1.0 wt%, **c** 1.5 wt%, and **d** 2.0 wt%

The HCE showed a relatively wide and strong absorption band in the vicinity of 3329 cm^{-1}, which appeared due to the stretching vibration of abundant hydroxyl functional groups. In addition, strong elastic vibrations of C–H and C–O absorption bands were observed around 2924 cm^{-1} and 1043 cm^{-1}. In HCE/PU nanofibers, the absorption bands of HCE at 3329 cm^{-1}, 2924 cm^{-1}, and 1043 cm^{-1} were overlapped with PU characteristics bands. In addition, in the bands of HCE/PU nanofibers at 0.5 and 1wt% of HCE addition, no changes in peak positioning and intensity were observed. As the concentration of HCE increases, the intensity of the spectrum at

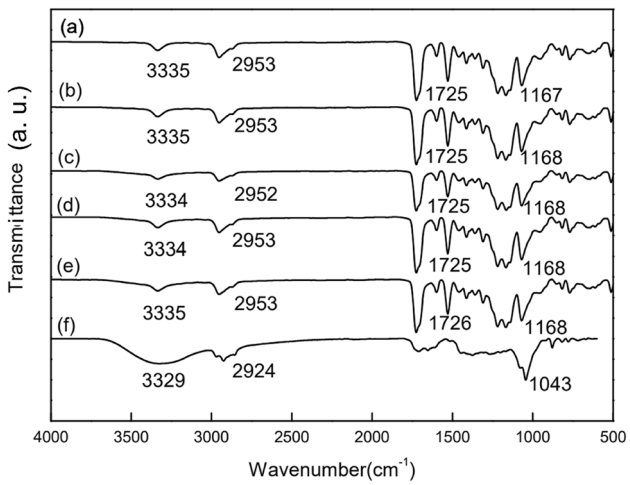

Fig. 5 FTIR spectra of the HCE/PU nanofibers with different HCE concentrations: (a) 0 wt%, (b) 0.5 wt%, (c) 1.0 wt%, (d) 1.5 wt%, (e) 2.0 wt%, and (f) as extracted HCE

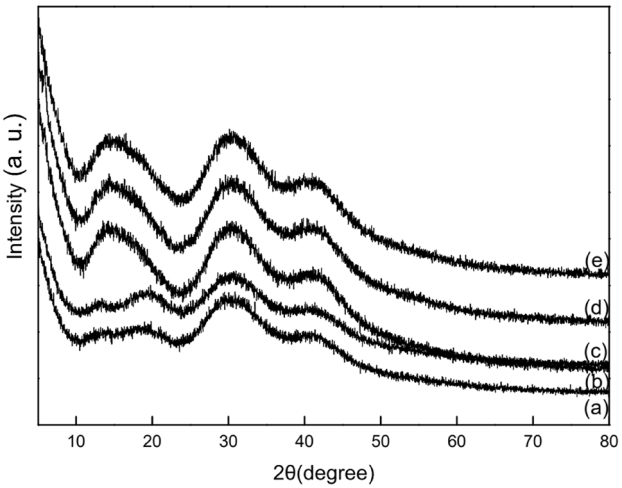

Fig. 6 XRD patterns of the HCE/PU nanofibers with different HCE concentrations: (a) 0 wt%, (b) 0.5 wt%, (c) 1.0 wt%, (d) 1.5 wt%, (e) 2.0 wt%

3334 cm^{-1} was slightly increased. This is due to the influence of the hydroxyl characteristics band of HCE thus demonstrating the successful incorporation of HCE in PU nanofibrous assemblies.

XRD analysis of PU/HCE nanofibers

The incorporation of any filler material in the nanofibrous structure causes a change in the crystallinity of the base polymer due to changes in the packing density incurred from filler-polymers interactions. The XRD analysis is a method of determining such changes in the crystal structure and crystallinity of a polymer. The HCE/PU nanofibers were subjected to XRD analysis to identify whether any changes occurred in PU polymers by the addition of HCE as depicted in Fig. 6. The pristine PU nanofibers display a strong diffraction peak at Bragg's angle, $2\theta = 30°$ with two shoulders at 18° and 41°. The peak at 18° represents the existence of a mixed ordered structure of both hard and soft domains and an amorphous phase of the PU matrix. The peaks at 30° and 41° represent the mixing part of hard and soft components of PU, respectively (Li et al., 2020). With the increment of HCE content in PU, the intensities of these diffraction peaks at 30° and 41° were increased obviously, which should correspond to the increasing content of the hard segment. A new diffraction peak at $2\theta = 14°$ may be indicating that new crystalline zones were formed (Xu et al., 2018). This seems to reflect the diffraction peak shape of the XRD spectrum of flavonoid components: quercitrin and quercetin from ethanol extracted *HCE* (Pool et al., 2012). The addition of *HCE* might improve the molecular packing of the PU matrix thus enhancing the crystallinity of HCE/PU nanofibers. The slight increase in the intensity of $2\theta = 14°$ also demonstrate increased loading of HCE in HCE/PU nanofibers. Besides, the appearance of diffractions bands corresponding to HCE-derived quercitrin and quercetin further demonstrated the incorporation of HCE in PU nanofibers.

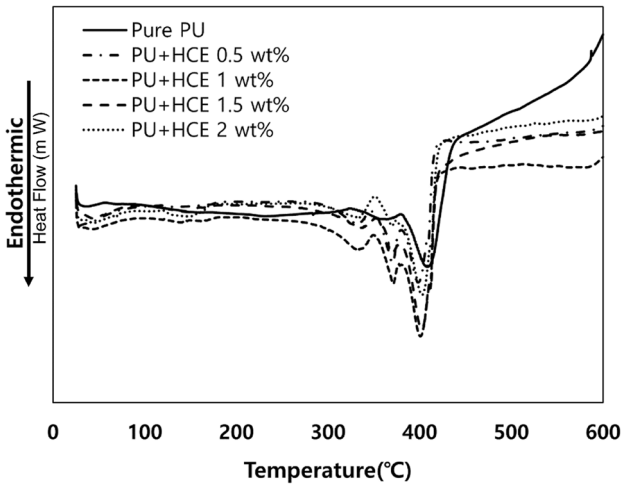

Fig. 7 DSC curves of pristine PU and HCE/PU nanofibers with different HCE concentrations

Thermal analysis of HCE/PU nanofibers

The incorporation of different functional compound in polymeric nanofibrous assembly affect the inherent properties of the resultant nanofibers, which may restrict its target application. The change incurred in the thermal property of our produced HCE/PU nanofibers provide an important information for its viability to be used as healthcare product such as-wound dressing material. The results of differential scanning calorimetry (DSC) of pristine PU and HCE/PU nanofibers are shown in Fig. 7. The melting temperature (T_m) of pristine PU was found at 409.39 ℃, while the HCE/PU nanofibers exhibited a reduction in melting temperatures, calculated to 398.54 ℃, 400.64 ℃, 401.98 ℃, and 402.69 ℃ with increased concentration of HCE in PU matrix. The melting points of the flavonoid components of HCE namely—quercitrin and quercetin are 182–185 ℃ and 325 ℃, respectively (Nguyen & Bechtold, 2021; Psimadas et al., 2012). Therefore, when ethanol extracted HCE was added, the melting temperature of the HCE/PU composite nanofibers reduced as compared to pristine PU nanofibers. Such findings demonstrate that the addition of HCE in PU nanofibrous structure although reduced the melting temperature of the PU to some extent, the change is not abnormal. A drastic and abnormal reduction in the melting temperature of a polymeric nanofiber-based dressing is an indication that the added active compound induced strong interruption in the polymeric chain, thereby causing to form an unsuitable and structurally unstable nanofibrous network to be used in wound surface. The enthalpy of the endothermic peak of pristine PU nanofibers was 270.05 J/g, but for 0.5 wt% and 1 wt% HCE-loaded PU nanofibers, the enthalpy of the endothermic peak was 383.85 J/g and 451.62 J/g, respectively. This means that the amount of heat (ΔHm) required for thermal decomposition of PU nanofibers increases as the amount of HCE concentration in the PU polymer matrix increases. Our XRD analysis also supports these findings. However, when 1.5 and 2 wt% HCE were added, the ΔHm slightly decrease thus indicating the reduction in energy requirements to melt

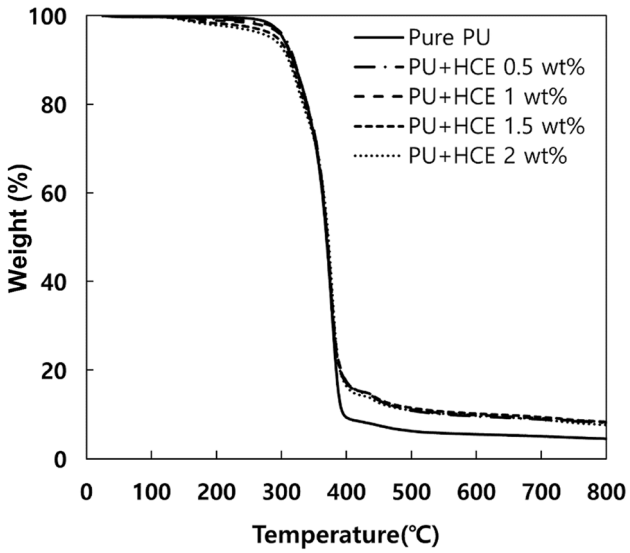

Fig. 8 Thermal degradation behavior of pristine PU and HCE/PU nanofibers with different HCE concentrations

HCE/PU nanofibers. This phenomenon can be described as the ethanol extracted HCE contained in PU polymer matrix, the essential oil components of HCE also increase, which act as a lubricant between the chain, thus reducing the bond-breaking energy.

Thermal excitation causes the covalent bonds in PU to undergo complex vibration and rotation within their local space. With the increase in degradation temperature, these covalent bonds break and form a variety of small molecules and fragment radicals. The mutual recombination of these small molecules and fragment radicals occurred or may undergo further fragmentation. Eventually, the resultant fragments vaporized or carbonized. The decomposition process stops with the loss of all volatile components and with char formation. The obtained char is composed of the crystalline and amorphous region, and carbon-containing polynuclear compounds with heteroatoms such as P, S, N, and O. The char may also contain inorganic residue from PU-contained heteroatoms and their presence can be identified either within the structure or as the result of additive incorporation (Coutinho & Delpech, 2000; Liaw, 1997 Zoran et al. 1994). Thermogravimetric analysis (TGA) was used to investigate the thermal stability of the HCE/PU nanofibers as graphically shown in Fig. 8. In general, the pyrolysis of polyurethane takes place in 2–3 steps, and the composition of the decomposed product depends on the structure of the PU polymer (Chattopadhyay & Webster, 2009). The thermal decomposition pattern of HCE/PU nanofibers did not alter even with the addition of HCE. No change in the weight (%) of PU and HCE/PU nanofibers was observed till 100 °C. This means the addition of HCE in PU polymeric nanofibers didn't change the moisture level of the nanofibers which is particularly a good parameter for a material to be used as wound dressing. If wound

dressing contains higher level of moisture, further successive absorption of moisture from wound fluid particularly in chronic wounds, an inhibitory action of wound healing is observed. The thermal decomposition of the PU nanofibers initiated at 268 °C and continued till 397 °C. Approx. 91% weight loss occurred within this temperature range. The addition of HCE slightly reduced the initial degradation temperatures of HCE/PU nanofibers. A linear reduction in degradation temperature was recorded with the increase in HCE concentrations. The degradation started at 228, 192, 157, and 149 °C for 0.5, 1, 1.5, and 2 wt% HCE incorporated PU nanofibers, respectively. However, although the decomposition initiation temperature decreases, this difference gradually disappears as the decomposition proceeds. The residual amount of PU nanofibers at 800 ℃ was 4.5%, but the residual amount of maximum HCE-loaded (2 wt%) PU nanofibers was 8.32%. The addition of ethanol extracted HCE increases the thermal stability of PU nanofibers at higher temperatures. The lower initial decomposition temperature and higher remaining weight (%) of PU/HCE than pure PU nanofibers were attributed to HCE in the PU nanofiber polymer matrix.

Conclusions

In this study, *Houttuynia cordata* was extracted using ethanol and distilled water as the solvent and the antioxidant components and antioxidant activities of the extracts were analyzed and discussed. After that HCE with the better antioxidant activity was added to PU polymer solution to make HCE/PU nanofibers via electrospinning. The morphology of the nanofiber was observed to evaluate appropriate HCE/PU fabrication conditions, and the physicochemical changes were analyzed to confirm the compatibility of PU and HCE. The total polyphenol and total flavonoid contents of the ethanol extracted HCE were both higher than those of the DW extracted HCE thus resulting in better antioxidant activity ethanol extracted HCE. At 12 wt% PU polymer concentration, uniform bead-free nanofibers having an average diameter of around 200 nm were formed with the addition of 1 and 1.5 wt% HCE. The analysis of FTIR, XRD, DSC, and TGA confirmed the successful incorporation of HCE in the PU matrix. Although the melting point was decreased by the influence of quercitrin and quercetin, which are the main polyphenol components of the HCE, the crystallinity, heat capacity, and thermal stability at high temperatures increased. Our findings confirmed that antioxidant HCE/PU nanofibers can be produced by electrospinning employing specific parameters. The ethanol extracted HCE owing to its high antioxidant activity is expected to be prepared in polymer nanofiber embedded form for a wide variety of healthcare applications.

Abbreviations

ABTS	2,2′-Azino-bis (3-ethylben zothiazoline-6-sulfonic acid) diammonium salt
DMF	Dimethylformamide
DPPH	2,2-Diphenyl-1-picrylhydrazyl
DSC	Differential scanning calorimetry
DW	Distilled water
FTIR	Fourier Transform Infrared
HC	*Houttuynia cordata*
HCE	*Houttuynia cordata* Extract
LDL	Low-density lipoprotein
Pt	Platinum
PU	Polyurethane

SEM Scanning electron microscope
TGA Thermogravimetric analysis
XRD X-ray diffraction

Acknowledgements
Not applicable.

Authors' contributions
MXC: Conceptualization, methodology, investigation, visualization, and data curation. MKH: Conceptualization, methodology, investigation, visualization, data curation, writing—original draft, writing—review and editing. J-SL, ISK: Validation, supervisor. All authors read and approved the final manuscript.

Authors' information
MXC received the Master degree from the Department of Clothing & Textiles, Chungnam National University, South Korea in 2020.
MKH is a Doctoral candidate of the Nano Fusion Technology Research Group, Institute for Fiber Engineering (IFES), Interdisciplinary Cluster for Cutting Edge Research (ICCER), Shinshu University, Japan.
ISK is a Professor of Nano Fusion Technology Research Group, Institute for Fiber Engineering (IFES), Interdisciplinary Cluster for Cutting Edge Research (ICCER), Japan.
JL is a Professor of Department of Clothing & Textiles, Chungnam National University, South Korea.

Funding
This work was supported by research fund of Chungnam National University.

Availability of data and materials
The datasets used and/or analysed during the current study are available from the corresponding author on reasonable request.

Declarations

Ethics approval and consent to participate
Not applicable.

Competing interests
The author declares no competing interests.

Received: 25 July 2022 Accepted: 1 February 2023
Published online: 05 May 2023

References

Akduman, C., Özgüney, I., & Kumbasar, E. P. A. (2016). Preparation and characterization of naproxen-loaded electrospun thermoplastic polyurethane nanofibers as a drug delivery system. *Materials Science and Engineering C, 64*, 383–390. https://doi.org/10.1016/j.msec.2016.04.005

Almetwally, A. A., El-Sakhawy, M., Elshakankery, M. H., & Kasem, M. H. (2017). Technology of nano-fibers: Production techniques and properties—critical review. *Journal of the Textile Association, 78*(1), 5–14.

Arai, T., Tanaka, M., & Kawakami, H. (2012). Porphyrin-containing electrospun nanofibers: Positional control of porphyrin molecules in nanofibers and their catalytic application. *ACS Applied Materials and Interfaces, 4*(10), 5453–5457. https://doi.org/10.1021/am3013664

Bravo, L. (1998). Polyphenols: Chemistry, dietary sources, metabolism, and nutritional significance. *Nutrition Reviews, 56*(11), 317–333. https://doi.org/10.1111/j.1753-4887.1998.tb01670.x

Brown, D. (1995). *Encyclopedia of herbs and their uses*. Dorling Kindersley.

Chattopadhyay, D. K., & Webster, D. C. (2009). Thermal stability and flame retardancy of polyurethanes. *Progress in Polymer Science (oxford), 34*(10), 1068–1133. https://doi.org/10.1016/j.progpolymsci.2009.06.002

Chevion, S., & Chevion, M. (2000). Antioxidant status and human health. Use of cyclic voltammetry for the evaluation of the antioxidant capacity of plasma and of edible plants. *Annals of the New York Academy of Sciences, 899*, 308–325. https://doi.org/10.1111/j.1749-6632.2000.tb06196.x

Choi, Y., Kim, M., Shin, J., Park, J., & Lee, J. (2003). The antioxidant activities of the some commercial teas. *Journal of the Korean Society of Food Science and Nutrition*. https://doi.org/10.3746/jkfn.2003.32.5.723

Chuysinuan, P., Chimnoi, N., Pattani, L., Khlaychan, P., Nooeaid, P., & Techasakul, S. (2017). Poly(lactic acid) (PLA) electrospun fibers containing rice extract: Release characteristics and their antioxidant activity. *Key Engineering Materials*. https://doi.org/10.4028/www.scientific.net/KEM.757.83

Coutinho, F. M. B., & Delpech, M. C. (2000). Degradation profile of films cast from aqueous polyurethane dispersions. *Polymer Degradation and Stability, 70*(1), 49–57. https://doi.org/10.1016/S0141-3910(00)00087-2

Da Silva, G. R., Da Silva Cunha, A., Ayres, E., & Oréfice, R. L. (2009). Effect of the macromolecular architecture of biodegradable polyurethanes on the controlled delivery of ocular drugs. *Journal of Materials Science: Materials in Medicine, 20*(2), 481–487. https://doi.org/10.1007/s10856-008-3607-y

Feng, S., Zhang, F., Ahmed, S., & Liu, Y. (2019). Physico-mechanical and antibacterial properties of PLA/TiO2 composite materials synthesized via electrospinning and solution casting processes. *Coatings, 9*(8), 525. https://doi.org/10.3390/coatings9080525

Fu, J., Dai, L., Lin, Z., & Lu, H. (2013). *Houttuynia cordata* Thunb: a review of phytochemistry and pharmacology and quality control. *Chinese Medicine, 04*(03), 101–123. https://doi.org/10.4236/cm.2013.43015
Gotmare, V. D., Kole, S. S., & Athawale, R. B. (2018). Sustainable approach for development of antimicrobial textile material using nanoemulsion for wound care applications. *Fashion and Textiles*. https://doi.org/10.1186/s40691-018-0138-0
Haider, M. K., Sun, L., Ullah, A., Ullah, S., Suzuki, Y., Park, S., Kato, Y., Tamada, Y., & Kim, I. S. (2021). Polyacrylonitrile/Carbon Black nanoparticle/Nano-Hydroxyapatite (PAN/nCB/HA) composite nanofibrous matrix as a potential biomaterial scaffold for bone regenerative applications. *Materials Today Communications, 27*, 102259. https://doi.org/10.1016/j.mtcomm.2021.102259
Halliwell, B. (1997). Antioxidants and human disease: A general introduction. *Nutrition Reviews, 55*(1), 44–52.
Hillis, W. E., & Swain, T. (1959). The phenolic constituents of Prunus domestica. II.—The analysis of tissues of the Victoria plum tree. *Journal of the Science of Food and Agriculture, 10*(2), 135–144. https://doi.org/10.1002/jsfa.2740100211
Jeong, C., Choi, S., & Heo, H. (2008). Analysis of nutritional components and evaluation of functional activities of *Sasa borealis* leaf tea. *Korean Journal of Food Science and Technology., 40*(5), 586–592.
Jeong, H. R., Kwak, J. H., Kim, J. H., Choi, G. N., Jeong, C., & Heo, H. J. (2010). Antioxidant and neuronal cell protective effects of an extract of *Houttuynia cordata* Thunb (a Culinary Herb). *Korean Journal of Food Preservation, 17*(5), 720–726.
Kim, J. W., Um, M., & Lee, J. W. (2018). Antioxidant activities of hot water extracts from different parts of rugosa rose (*Rosa rugosa* thunb.). *Journal of the Korean Wood Science and Technology, 46*(1), 38–47. https://doi.org/10.5658/WOOD.2018.46.1.38
Kwak, H. W., Woo, H., Kim, I. C., & Lee, K. H. (2017). Fish gelatin nanofibers prevent drug crystallization and enable ultrafast delivery. *RSC Advances, 7*(64), 40411–40417. https://doi.org/10.1039/c7ra06433k
Lee, I. W., Li, J., Chen, X., & Park, H. J. (2017). Fabrication of electrospun antioxidant nanofibers by rutin-pluronic solid dispersions for enhanced solubility. *Journal of Applied Polymer Science, 134*(21), 1–10. https://doi.org/10.1002/app.44859
Li, B., Liu, Y., Wei, S., Huang, Y., Yang, S., Xue, Y., Xuan, H., & Yuan, H. (2020). A solvent system involved fabricating electrospun polyurethane nanofibers for biomedical applications. *Polymers, 12*(12), 1–12. https://doi.org/10.3390/polym12123038
Li, J., Shu, Y., Hao, T., Wang, Y., Qian, Y., Duan, C., Sun, H., Lin, C., & Wang, C. (2013). A chitosan-glutathione based injectable hydrogel for suppression of oxidative stress damage in cardiomyocytes. *Biomaterials, 34*(36), 9071–9081. https://doi.org/10.1016/j.biomaterials.2013.08.031
Liaw, D. J. (1997). The relative physical and thermal properties of polyurethane elastomers: Effect of chain extenders of bisphenols, diisocyanate, and polyol structures. *Journal of Applied Polymer Science, 66*(7), 1251–1265. https://doi.org/10.1002/(SICI)1097-4628(19971114)66:7%3c1251::AID-APP5%3e3.0.CO;2-F
Moreno, M. I. N., Isla, M. I., Sampietro, A. R., & Vattuone, M. A. (2000). Comparison of the free radical-scavenging activity of propolis from several regions of Argentina. *Journal of Ethnopharmacology, 71*(1–2), 109–114. https://doi.org/10.1016/S0378-8741(99)00189-0
Nguyen, H. L., & Bechtold, T. (2021). Thermal stability of natural dye lakes from Canadian Goldenrod and onion peel as sustainable pigments. *Journal of Cleaner Production, 315*, 128195. https://doi.org/10.1016/j.jclepro.2021.128195
Petrovic, Z. S., Zavargo, Z., Flynn, J. H., & Macknight, W. J. (1994). Thermal Degradation of Segmented Polyurethanes. *Journal of Applied Polymer Science, 51*, 1087–1095.
Pool, H., Quintanar, D., Figueroa, J. D. D., Marinho Mano, C., Bechara, J. E. H., Godínez, L. A., & Mendoza, S. (2012). Antioxidant effects of quercetin and catechin encapsulated into PLGA nanoparticles. *Journal of Nanomaterials*. https://doi.org/10.1155/2012/145380
Psimadas, D., Georgoulias, P., Valotassiou, V., & Loudos, G. (2012). Molecular nanomedicine towards cancer. *Journal of Pharmaceutical Sciences, 101*(7), 2271–2280. https://doi.org/10.1002/jps
Pusporini, P., Edikresnha, D., Sriyanti, I., Suciati, T., Munir, M. M., & Khairurrijal, K. (2018). Electrospun polyvinylpyrrolidone (PVP)/green tea extract composite nanofiber mats and their antioxidant activities. *Materials Research Express, 5*(5), 054001. https://doi.org/10.1088/2053-1591/aac1e6
Sriyanti, I., Edikresnha, D., Rahma, A., Munir, M. M., Rachmawati, H., & Khairurrijal, K. (2017). Correlation between structures and antioxidant activities of polyvinylpyrrolidone/*Garcinia mangostana* L. extract composite nanofiber mats prepared using electrospinnin. *Journal of Nanomaterials*. https://doi.org/10.1155/2017/9687896
Ullah, A., Saito, Y., Ullah, S., Haider, M. K., Nawaz, H., Duy-Nam, P., Kharaghani, D., Kim, I. S., et al. (2021). Bioactive Sambong oil-loaded electrospun cellulose acetate nanofibers: Preparation, characterization, and in-vitro biocompatibility. *International Journal of Biological Macromolecules, 166*, 1009–1021. https://doi.org/10.1016/j.ijbiomac.2020.10.257
Unnithan, A. R., Sasikala, A. R. K., Murugesan, P., Gurusamy, M., Wu, D., Park, C. H., & Kim, C. S. (2015). Electrospun polyurethane-dextran nanofiber mats loaded with Estradiol for post-menopausal wound dressing. *International Journal of Biological Macromolecules, 77*, 1–8. https://doi.org/10.1016/j.ijbiomac.2015.02.044
Woo, H. W., & Lee, J. S. (2021). Characterization of electrospun *Aronia melanocarpa* fruit extracts loaded polyurethane nanoweb. *Fashion and Textiles*. https://doi.org/10.1186/s40691-021-00250-z
Xu, W., Xiao, M., Yuan, L., Zhang, J., & Hou, Z. (2018). Preparation, physicochemical properties and hemocompatibility of biodegradable chitooligosaccharide-based polyurethane. *Polymers, 10*(6), 1–17. https://doi.org/10.3390/polym10060580
Xu, X., Ye, H., Wang, W., Yu, L., & Chen, G. (2006). Determination of flavonoids in *Houttuynia cordata* Thunb. and *Saururus chinensis* (Lour.) Bail by capillary electrophoresis with electrochemical detection. *Talanta, 68*(3), 759–764. https://doi.org/10.1016/j.talanta.2005.05.027
Yang, Z., Peng, H., Wang, W., & Liu, T. (2010). Crystallization behavior of poly(ε-caprolactone)/layered double hydroxide nanocomposites. *Journal of Applied Polymer Science, 116*(5), 2658–2667. https://doi.org/10.1002/app
Yang, W., Sousa, A. M. M., Thomas-Gahring, A., Fan, X., Jin, T., Li, X., et al. (2016). Electrospun polymer nanofibers reinforced by tannic acid/Fe+++ complexes. *Materials, 9*(9), 1–12. https://doi.org/10.3390/ma9090757
Zhou, B., Hu, X., Zhu, J., Wang, Z., Wang, X., & Wang, M. (2016). Release properties of tannic acid from hydrogen bond driven antioxidative cellulose nanofibrous films. *International Journal of Biological Macromolecules, 91*, 68–74. https://doi.org/10.1016/j.ijbiomac.2016.05.084